Heliyon 11 (2025) e42445

Contents lists available at ScienceDirect

Heliyon

journal homepage: www.cell.com/heliyon

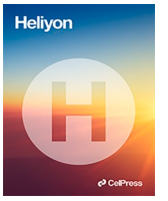

Research article

A bird's eye view to the homeostatic, Alzheimer and Glioblastoma attractors

Joan Nieves *, Gabriel Gil, Augusto Gonzalez

Institute of Cybernetics, Mathematics and Physics, Havana, Cuba

ARTICLE INFO

Keywords:
Gene expression space
White matter of the brain
Aging
Glioblastoma
Alzheimer's disease

ABSTRACT

Dimensional reduction analysis of available data for white matter of the brain allows to locate the normal (homeostatic), Glioblastoma and Alzheimer's disease attractors in gene expression space and to identify paths related to transitions like carcinogenesis or Alzheimer's disease onset. A predefined path for aging is also apparent, which is consistent with the hypothesis of programmatic aging. In addition, reasonable assumptions about the relative strengths of attractors allow to draw a schematic landscape of fitness: a Wright's diagram. These simple diagrams reproduce known relations between aging, Glioblastoma and Alzheimer's disease, and rise interesting questions like the possible connection between programmatic aging and Glioblastoma in this tissue. We anticipate that similar multiple diagrams in other tissues could be useful in the understanding of the biology of apparently unrelated diseases or disorders, and in the discovery of unexpected clues for their treatment.

1. Introduction

A well known paradigm in molecular genetics expresses that local maxima of fitness in gene expression space are related to biological viable states [1]. This picture has been applied to the description of cell fates along differentiation lines [2]. However, to the best of our knowledge, there are no plots based on real data for a given tissue representing at least a partial landscape with more than two of these maxima. In the present paper, we provide a drawing for white matter of the brain in which the normal state (N) is represented along with the glioblastoma (GB) attractor and the seemingly modest maximum related to Alzheimer's disease (AD).

The plot shows that aging is a common risk factor for GB and AD and, at the same time, that GB and AD are opposite alternatives, as epidemiological [3–6] and molecular biology studies [7–9] suggest. The plot indicates also a path or corridor for normal aging, in accordance with the programmatic aging theory [10,11].

At the gene level, there are genes varying in the same way in the aging, AD progression and cancer processes, whereas there are also genes indicating the disjunctive between AD and GB. An example of the latter is the MMP9 protein-coding gene, playing an important role in tumor invasion [12,13], but known also as a neuroprotector, controlling the interactions between axons and beta-amyloid fibers [14]. Deviations of the gene expression value from its reference in normal tissue may indicate either a potential progression to AD (under-expression) or to GB (over-expression).

This unusual view, following from a simple plot, may help understand the relations between AD and GB biology and identify useful gene markers for both processes. As an extra bonus, the plot allows to rise very interesting questions which are to be discussed below.

* Corresponding author.
E-mail address: joan.nieves@icimaf.cu (J. Nieves).

https://doi.org/10.1016/j.heliyon.2025.e42445
Received 21 February 2024; Received in revised form 14 January 2025; Accepted 3 February 2025
Available online 4 February 2025

1.1. The N + GB + AD diagram

Our starting point is the principal component analysis [15] diagram of gene expression data for white matter of the brain, shown in Fig. 1a). As noticed in the figure, the first two principal components, PC1 and PC2 axes in the figure, capture more than 80 % of the variance in the dispersion of points. Thus, it is a fair two-dimensional representation of the actual distribution of points in gene expression space.

Four groups of samples are apparent in this figure. Samples labeled as N and GB correspond, respectively, to pathologically normal and tumor specimens in The Cancer Genome Atlas data for Glioblastoma (TCGA, https://www.cancer.gov/tcga) [16]. They are taken during surgery procedures. Tumors are geographically localized in different brain zones but, as it is common for Glioblastoma, they are white matter tumors [17]. The centers of the N and GB clouds of samples in gene expression space define, respectively, the Normal (homeostatic) and Glioblastoma Kauffman attractors [18,19]. Indeed, the accumulation of points in a certain region of this space indicates that this region is an attractor of the Gene Regulatory Network governing the dynamics.

There are 5 N samples from patients in the age range between 49 and 74 years, whereas in the 169 GB samples the age interval is between 21 and 89 years. Female patients approximately accounts for two thirds of the cohort.

On the other hand, the groups labeled as AD and O correspond, respectively, to Alzheimer's disease and control (old) white matter samples in the longitudinal Allen Institute study on aging and dementia (http://aging.brain-map.org/) [20]. They are taken post mortem. The O group is conformed by 47 samples, whereas there are 28 AD samples. The age interval for all of these samples is between 77 and 101 years. AD diagnostic is supported by cognitive and other clinical tests. Around 40 % of the cohort are female patients.

We studied the O to AD transition in Ref. [21]. In Fig. 4 of that reference it is shown that as age increases we observe a displacement of O samples towards the center of the AD cloud. However, the average position of the AD center does not depend on age. This property suggests that the center of the AD cloud of samples also defines an attractor in gene expression space. The O samples seem to be captured by the AD attractor in the process of aging.

As mentioned, we use gene expression data, in FPKM format, from Refs. [16,20]. The data was obtained by using different

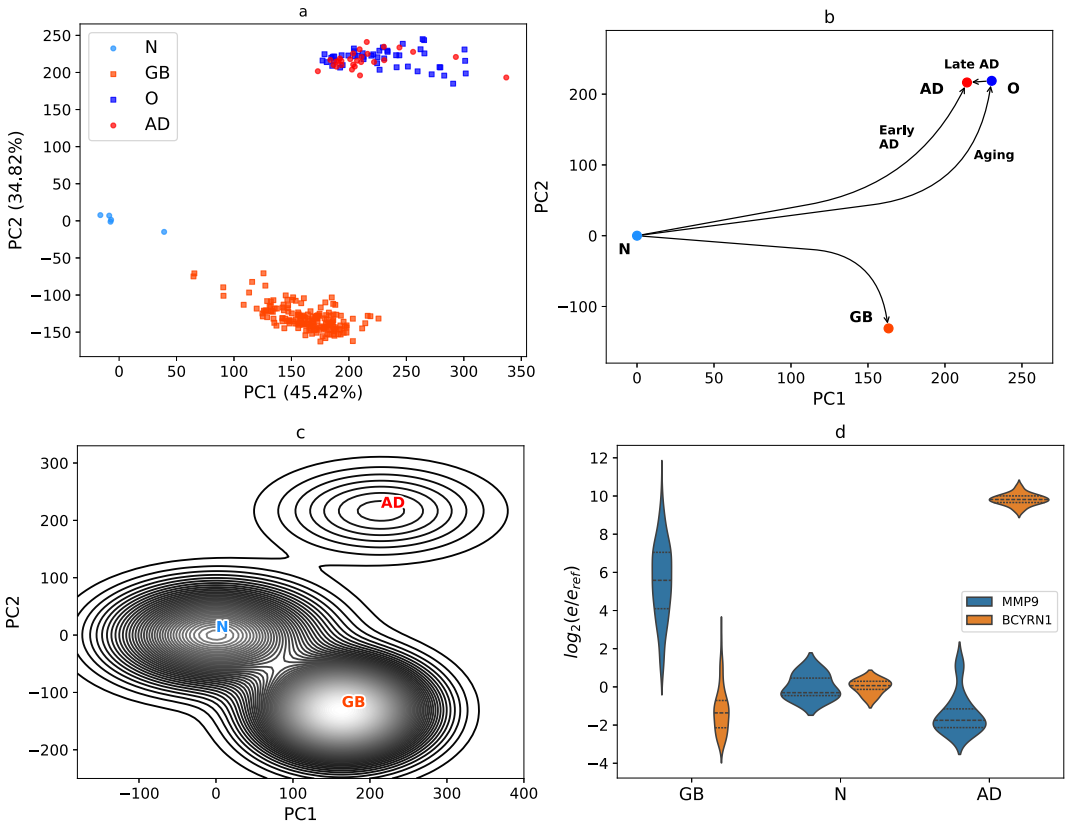

Fig. 1. Gene expression diagrams and schematic fitness landscape.
a) Principal component analysis of the data studied in the paper. N – Normal homeostatic state, GB – Glioblastoma, AD – Alzheimer's disease state. The normal old samples are denoted by O. **b)** Schematics of the transitions between attractors. **c)** A Wright diagram showing a hypothetical contour plot of fitness. The absolute maximum corresponds to the GB state. The AD attractor is represented as a slight local maximum. **d)** Violin plot for the log-fold changes of MMP9 and BCYRN1 genes in N, AD and GB states. The geometric mean of the expression in the N state is taken as reference in order to compute differential expression values.

platforms. We took the approximately 30,000 genes that are perfectly identified in both platforms and perform a simple Principal Component Analysis (PCA) [15], described elsewhere [19,21]. The common reference used to define log-fold differential expression values and compute the covariance matrix for the PCA is the geometric mean in the N state.

There are both conceptual and technical issues arising when using data from these two dissimilar experiments in a single PCA calculation. For example, the reference N is not precisely the normal brain state, but a set of pathologically normal samples taken from individuals with GB tumors. Two of the patients are even older than 70 years. From the computational side, on the other hand, one could use batch corrections [22,23], which partially amend the biases associated to each group of samples, but may introduce also uncontrolled artifacts.

Instead of introducing sophistication and uncontrolled artifacts, we directly take the data from the sources and use the simplest PCA technique. We don't believe that any correction will essentially change the qualitative analysis following from the 3-attractors diagrams shown in Fig. 1a).

The ideal situation would be to repeat the study within a single technological framework, to include data from young normal people, which should be used to set the reference for differential gene expression calculations, to include data from GB and AD patients, and data for normal patients in different age ranges. This is a complicated experiment, but it could be particularly feasible in a mouse model [24], for example. We look at our Fig. 1a) diagram as a qualitative approximation to this ideal experiment.

Thus, in our approximation we get a gene expression space landscape with 3 attractors: N, GB and AD, and a set of O samples moving towards the latter. The relative positions and main transitions between attractors are summarized in Fig. 1b). We assume that they are determined by the biology underlying the processes in the tissue. The N to AD transition is labeled as "early onset of AD" in order to stress that there is also a way to AD through aging, the "late onset of AD". A path for aging is also indicated in the figure. We shall come back to this point below.

1.2. Fitness landscape

There is still an additional qualitative information which can be introduced in our description. It is related to a fitness variable, in such a way that we draw a kind of Wright's diagram [1]. A schematic drawing containing a contour plot of fitness is represented in Fig. 1c). The N and GB attractors are fitness maxima, and they should be separated by a low-fitness barrier [21]. The GB should be the highest maximum [21,25]. On the other hand, the transition from O to AD is quasi-continuous, with a relatively small number of differentially expressed genes [21]. It means that there is a very small barrier or even a barrier-free path connecting O and AD. We expect a low-fitness barrier preventing the direct transitions from N to AD, and a small AD maximum, as this attractor is located in the far from N low-fitness region. All of these facts are represented in Fig. 1c). The scheme is constructed from a sum of Gaussians centered at the attractors, with standard deviations proportional to the actual values observed in Fig. 1a), and with heights qualitatively respecting the relative strengths of attractors.

Let us stress the meaning of a Wright's diagram in a brain tissue. In other tissues somatic evolution is mainly related to stem cell replications. But, in its normal state, brain is a very slowly replicating tissue [26]. Changes in small brain regions, that is displacements in the diagram, are basically accumulated damages, i.e. aging [27]. However, once the transition to the GB state occurs, there is an enormous increase of the replication rate of tumor cells. Let us, additionally, notice that changes related to aging are strongly apparent in white matter [28].

2. Main results

On the basis of our diagrams, we may formulate the following remarks or statements, which are the main results of the paper.

1. **There is a direction in gene expression space, which roughly speaking may be identified with the PC1 axis, associated with aging and with an increase in the risk for AD and GB.**

Indeed, displacement along this direction implies partially climbing the low-fitness barriers separating N from the AD and GB states, and thus augmenting the risk for both AD and GB.

It is worth looking at the main genes involved in this process. To this end, we look at the unitary vector along the PC1 axis. Genes are ranked according to their contribution to the unitary vector. The procedure is similar to the Page Rank algorithm [29]. We used it in our previous work [19].

A list with the first 100 genes in the ranking is given in Supplementary Table I. Positive amplitudes defines genes which expression increases in the displacement along the positive direction of PC1, whereas negative amplitudes refer to silenced genes. These genes should simultaneously play a crucial role in aging, GB and AD.

Of course, due to the qualitative-only value of our analysis the genes, and specially the ranking, should be taken with care. Nevertheless, notice that 20 of the silenced genes are related to the Transmission across chemical synapses pathway. In Supplementary Table II we list the main Reactome pathways associated to these genes [30]. There are 56 annotated genes in this set.

Decreased synaptic function is a known feature of the aged brain, according to the review [31]. The second main characteristic, according to this reference, is an increased immune function, which is not particularly apparent in our set of genes. Instead, we observe genes related to Neurotoxicity of clostridium toxins [32], to a decrease of mitochondria activity [33], micro RNAs shared between AD and GB [34], etc.

2. **There is a direction in gene expression space, which may be roughly identified with the PC2 axis, showing that AD and GB are excluding alternatives.**

Indeed, AD and GB seem to be in opposite semiplanes. Clinical evidence [3–6] and molecular biology studies [7–9] support this disjunctive. Consequently, the PC2 axis involves genes inversely deregulated in AD and GB.

In Supplementary Table III, we list the top 100 genes defined by the unitary vector along the PC2 axis. Positive weights correspond to genes which expression increases in the N to AD transition. On the other hand, negative amplitudes correspond to genes with increasing expression in the N to GB transition.

The Reactome pathways related to these genes are seen in Supplementary Table IV. They are mainly related to control of the cell cycle, DNA replication, apoptosis, modification of the extracellular matrix, etc, i.e. to cancer hallmarks [35–37].

Above, we mentioned MMP9 as an example of genes playing opposite roles in GB and AD. The UBE2C protein-coding gene is another known gene with this characteristic [38,39]. On the other hand, the RNA gene BCYRN1, also among the first 100 genes in the ranking, seems to be under-expressed in GB [40] and over-expressed in AD [41]. Fig. 1d) shows violin plots for the differential expression of both MMP9 and BCYRN1 genes in N, AD and GB samples.

Notice also that in Supplementary Table III there are many ribosome protein-coding, small nuclear, micro RNA and other genes, inversely regulated in both processes. Only 18 of the genes set are annotated in Reactome pathways. This is a usual problem with pathway analysis, where the biological functions of many genes are not annotated.

3. **There is an aging corridor, that is a preferential path for aging in gene expression space.**

In our data, there are samples in the N region and samples corresponding to normal aged brains, located in a definite region close to the AD attractor. In other words, the process of aging seems to define a trajectory or corridor of continuously decreasing fitness, from which the O data shows the last segment.

Samples in the intermediate region are, however, lacking.

Instead of including additional samples to our figure, which would introduce additional batch effects, we use recent results in a mouse model [24] showing undoubtedly a continuous corridor for aging. We give in Supplementary Fig. 1 a replot of their data for corpus callosum, a white matter rich region. In the left panel, the first two principal components are plotted for the centers of the subgroups of samples. Mouse ages between 3 and 28 months are considered, the latter is roughly equivalent to 80 years in a human scale. A corridor for aging is apparent. The right panel, on the other hand, shows true distances including all the components. Thus, the projections into the (PC1, PC2) plane are a fair representation of the actual distribution of points.

In our scheme, Fig. 1b), an aging corridor is delineated. Fig. 1c) suggests that the corridor is a direction with minimal decrease of fitness.

A preferential direction or corridor for aging is consistent with the hypothesis of programmatic aging [10,11], i.e. the idea that aging is programmed in our genes.

4. **The predetermined aging corridor could be related to the pressure of avoiding the strong GB attractor.**

A very interesting question to answer concerns the selection of a preferred direction for aging. Our oversimplified scheme Fig. 1c) offers an unexpected answer to this question: in white matter it could be related to the pressure of avoiding the strongest GB attractor.

Indeed, for each small portion of the tissue, one may model aging as a kind of random motion starting in the N region. Notice that a model of random jumps in gene expression space was used in Ref. [42] in order to describe somatic evolution of different tissues towards cancer. We first assume that the direction of jumps is random in the plane shown in Fig. 1c).

There are only four possibilities for the fate of random trajectories in the plane which start in the N region. First, the trajectory remains in the N region. Second, it arrives to a very low fitness region and the cells die. This is the fate of many cells in the old brain. Third, it is captured by the GB attractor. And, finally, the fourth possibility is the capture by the AD attractor.

Because of the huge basin of the GB attractor, there should be a relatively high probability for trajectories to be captured by the GB, leading to the initiation of a tumor. This implies an enormous increase of fitness, the spread of the tumor in brain and a life expectancy for the individual of only around two years after initiation [43]. It may impact on individuals in the reproductive age. Thus, avoiding the GB attractor could be the subject of selection pressure.

As an indirect check, we may compare GB and AD incidences. They should be proportional to the capture rates of random trajectories by the GB and AD attractors. As mentioned, in a model where the direction of jumps is random, the incidence of GB should be much higher than that of AD. However, global incidence for Glioblastoma is less than 10 in 100,000 people [44], as contrasted with the 5 % of AD for people in the 65–74 years age interval, and 13 % of people in the range from 75 to 84 years [45]. The observed incidence suggests that the motion towards the GB center is avoided.

5. **The late onset of AD could the result of capture by the AD attractor of aged brain micro states.**

The picture is, thus, as follows. The process of aging is initially related to a displacement along the aging corridor with the corresponding decrease of fitness. In the last steps, the O states are captured by the weak AD attractor.

As mentioned above, the statement about the aging corridor is supported by the experiment in a mouse model, whereas the capture by the AD center is suggested by calculations in Ref. [21], particularly by the results shown in Fig. 4 of that reference.

In Supplementary Table V we show the top 10 genes in the O to AD transition. They involve genes included in the Supplementary Table I, but varying in the opposite direction, that is in the negative direction of the PC1 axis. This fact is represented in the schematic diagram given in Fig. 1b).

3. Discussion

Our simple qualitative drawings identify directions in gene expression space associated to different biological processes: aging, carcinogenesis, AD onset. Everyone of these directions is characterized by a "metagene" or gene expression profile, from which the main genes contributing to the process can be extracted.

Some of our results confirm previous knowledge, but others require further corroborations. For example, the idea that programmatic aging could be related to avoiding the strongest GB attractor, or the late onset of AD as the capture by the AD attractor of normal aged samples. We hope, they will motivate experimental research work along these directions. Particularly feasible is the experiment in a mouse model, a nice example of which is Ref. [24].

Let us stress that even more refined data or computational methods could not essentially modify our qualitative schemes with only 3 attractors. Their relative positions could vary, but the formulated statements will remain.

Because of the qualitative character of our study, the analysis of relevant genes and pathways is not properly addressed in the paper. Let us, however, qualitatively look at seven known markers for AD and GB on the basis of our scheme. Violin plots for these genes are shown in Supplementary Fig. 2. The figure shows that the MAPT (tau protein [46]) and APP (amyloid beta [47]) genes are under-expressed in both GB and AD and, thus, according to our scheme are PC1-like genes, mainly related to aging. In a certain way, this is consistent with findings by the Allen Institute study concerning the patterns of tau protein and amyloid plaques in the aged brain. Of course, certain mutations of these genes could lead to accelerated brain aging and early onset of AD. The APOE gene [48], on the contrary, is inversely deregulated in GB and AD. It is a PC2-like gene.

On the other hand, the IDH1 marker [49] is over-expressed in GB, but it is irrelevant in AD. The three GB markers IDH2 [49], MKI67 [50] and ATRX [51] are PC2-like genes. They have been mainly studied in connection with GB, but the fact that they are PC2 genes indicates that they could possibly play an important role in AD also.

Let us consider, as a final example, the recent demonstration of the relevance of TREM2 in AD [52]. Activating TREM2 in AD is shown to enhance microglial metabolism. According to our analysis, TREM2 is a PC2 gene, under-expressed in AD and over-expressed in GB. Thus, we expect that knocking down TREM2 in glioma cells could have an important effect on GB. This fact, following from our simple scheme, is presently under study [53].

The diagram in Fig. 1a) should be completed with data corresponding to other kinds of dementia or brain disorders. In particular, one should expect a Parkinson disease area close to the AD attractor and opposite to GB [54]. The whole picture may reveal a still finer topology of gene expression space and a richer Wright diagram.

We anticipate that similar diagrams in other tissues, besides providing an integral perspective, could be useful in the understanding of the biology of apparently unrelated diseases or disorders, and in the discovery of unexpected clues for their treatment.

4. Limitations of the study

The main limitation was already mentioned: data is insufficient and imperfect. We, nevertheless, strongly believe that conclusions deriving from our qualitative three-attractors diagrams are robust against data improvement. Additional testing in a mouse model, along the same lines of the experiment shown in Ref. [24], is feasible and highly desirable.

CRediT authorship contribution statement

Joan Nieves: Writing – review & editing, Visualization, Software, Investigation, Formal analysis, Data curation. **Gabriel Gil:** Writing – review & editing, Supervision, Investigation, Formal analysis. **Augusto Gonzalez:** Writing – review & editing, Writing – original draft, Validation, Supervision, Project administration, Investigation, Formal analysis, Conceptualization.

Availability of data and code

The data we used, the Python routines and the main results are integrated in the following public GitHub repository: https://github.com/JoanANievesCuadrado/GB_vs_AD.

Declaration of competing interest

The authors declare that they have no known competing financial interests or personal relationships that could have appeared to influence the work reported in this paper.

Acknowledgments

Authors acknowledge the Office of External Activities of the Abdus Salam Centre for Theoretical Physics for support. The research is carried on under a project of the Nuclear Energy and Advanced Technologies Agency (AENTA), Cuba. Authors are grateful to C.

Carricarte and R. Perez for a critical reading of the manuscript.

Appendix A. Supplementary data

Supplementary data to this article can be found online at https://doi.org/10.1016/j.heliyon.2025.e42445.

References

[1] Sewall Wright, The roles of mutation, inbreeding, crossbreeding and selection in evolution, Proceedings of the 6th International Congress on Genetics 1 (1932) 356–366.
[2] M.J. Casey, P.S. Stumpf, B.D. MacArthur, Theory of cell fate, WIREs Systems Biology and Medicine 12 (2019) e1471.
[3] S.-M. Ou, et al., Does Alzheimer's disease protect against cancers? A nationwide population-based study, Neuroepidemiology 40 (2012) 42–49.
[4] J.A. Driver, et al., Inverse association between cancer and Alzheimer's disease: results from the Framingham Heart Study, BMJ 344 (2012) e1442.
[5] C.M. Roe, et al., Cancer linked to Alzheimer's disease but not vascular dementia, Neurology 74 (2009) 106–112.
[6] M. Musicco, et al., Inverse occurrence of cancer and Alzheimer's disease: a population-based incidence study, Neurology 81 (2013) 322–328.
[7] T. Liu, et al., Transcriptional signaling pathways inversely regulated in Alzheimer's disease and glioblastoma multiform, Sci. Rep. 3 (2013) 3467.
[8] C. Lanni, M. Masi, M. Racchi, S. Govoni, Cancer and Alzheimer's disease inverse relationship: an age-associated diverging derailment of shared pathways, Mol. Psychiatr. 26 (2020) 280–295.
[9] J. Cai, et al., Exploring the inverse association of glioblastoma multiforme and Alzheimer's disease via bioinformatics analysis, Med. Oncol. 39 (2022) 182.
[10] J.P. de Magalhães, Programmatic features of aging originating in development: aging mechanisms beyond molecular damage? FASEB J. 26 (2012) 4821–4826.
[11] D. Gems, The hyperfunction theory: an emerging paradigm for the biology of aging, Ageing Res. Rev. 74 (2022) 101557.
[12] G. Choe, et al., Active matrix metalloproteinase 9 expression is associated with primary glioblastoma subtype, Clin. Cancer Res. 8 (2002) 2894–2901.
[13] Q. Xue, et al., High expression of MMP9 in glioma affects cell proliferation and is associated with patient survival rates, Oncol. Lett. 13 (2017) 1325–1330.
[14] A. Kaminari, N. Giannakas, A. Tzinia, E.C. Tsilibary, Overexpression of matrix metalloproteinase-9 (MMP-9) rescues insulin-mediated impairment in the 5XFAD model of Alzheimer's disease, Sci. Rep. 7 (2017) 683.
[15] J. Lever, M. Krzywinski, N. Altman, Principal component analysis, Nat. Methods 14 (2017) 641–642.
[16] C. Brennan, et al., The somatic genomic landscape of glioblastoma, Cell 155 (2013) 462–477.
[17] B.M. Ellingson, et al., Probabilistic radiographic Atlas of glioblastoma phenotypes, Am. J. Neuroradiol. 34 (2012) 533–540.
[18] S. Huang, I. Ernberg, S. Kauffman, Cancer attractors: a systems view of tumors from a gene network dynamics and developmental perspective, Semin. Cell Dev. Biol. 20 (2009) 869–876.
[19] A. Gonzalez, D.A. Leon, Y. Perera, R. Perez, On the gene expression landscape of cancer, PLoS One 18 (2023) e0277786.
[20] J.A. Miller, et al., Neuropathological and transcriptomic characteristics of the aged brain, Elife 6 (2017) 31126.
[21] A. Gonzalez, J. Nieves, D.A. Leon, M.L. Bringas Vega, P.V. Sosa, Gene expression rearrangements denoting changes in the biological state, Sci. Rep. 11 (2021) 8470.
[22] L. Haghverdi, A. Lun, M. Morgan, et al., Batch effects in single-cell RNA-sequencing data are corrected by matching mutual nearest neighbors, Nat. Biotechnol. 36 (2018) 421–427.
[23] Y. Zhang, G. Parmigiani, W.E. Johnson, *ComBat-seq*: batch effect adjustment for RNA-seq count data, NAR Genom. Bioinform 2 (2020) lqaa078.
[24] Oliver Hahn, Aulden G. Foltz, Micaiah Atkins, et al., Atlas of the aging mouse brain reveals white matter as vulnerable foci, Cell 186 (2023) 4117–4133, https://doi.org/10.1016/j.cell.2023.07.027.
[25] A. Gonzalez, F. Quintela, D.A. Leon, M.L. Bringas-Vega, P.A. Valdes-Sosa, Estimating the number of available states for normal and tumor tissues in gene expression space, Biophysical Reports 2 (2022) 100053.
[26] Kirsty L. Spalding, Ratan D. Bhardwaj, Bruce A. Buchholz, et al., Retrospective birth dating of cells in humans, Cell 122 (2005) 133–142.
[27] B. Schumacher, J. Pothof, J. Vijg, et al., The central role of DNA damage in the ageing process, Nature 592 (2021) 695–703, https://doi.org/10.1038/s41586-021-03307-7.
[28] C.R.G. Guttmann, F.A. Jolesz, R. Kikinis, et al., White matter changes with normal aging, Neurology 50 (1998) 972–978.
[29] N. Duhan, A.K. Sharma, K.K. Bhatia, Page ranking algorithms: a survey, in: 2009 IEEE International Advance Computing Conference, 2009, pp. 1530–1537, https://doi.org/10.1109/iadcc.2009.4809246.
[30] Marc Gillespie, Bijay Jassal, Ralf Stephan, et al., The reactome pathway knowledgebase, Nucleic Acids Res. 50 (2022) D687–D692, 2022.
[31] S. Ham, S.J.V. Lee, Advances in transcriptome analysis of human brain aging, Exp. Mol. Med. 52 (2020) 1787–1797.
[32] M. Biazzo, M. Allegra, G. Deidda, Clostridioides difficile and neurological disorders: new perspectives, Frontiers in Neurosciences 16 (2022) 946601.
[33] Nuo Sun, Richard J. Youle, Toren Finkel, The mitochondrial basis of aging, Mol. Cell 61 (2016) 654–666.
[34] L. Thomas, T. Florio, C. Perez-Castro, Extracellular vloaded miRNAs as potential modulators shared between glioblastoma, and Parkinson's and Alzheimer's diseases, Front. Cell. Neurosci. 14 (2020) 590034.
[35] D. Hanahan, R.A. Weinberg, The hallmarks of cancer, Cell 100 (2000) 57–70.
[36] D. Hanahan, R.A. Weinberg, Hallmarks of cancer: the next generation, Cell 144 (2011) 646–674.
[37] D. Hanahan, Hallmarks of cancer: new dimensions, Cancer Discov. 12 (2022) 31–46.
[38] R. Ma, et al., High expression of UBE2C is associated with the aggressive progression and poor outcome of malignant glioma, Oncol. Lett. 11 (2016) 2300–2304.
[39] S.K. Jaladanki, A. Elmas, G.S. Malave, K. Huang, Genetic dependency of Alzheimer's disease-associated genes across cells and tissue types, Sci. Rep. 11 (2021) 12107.
[40] M. Mu, W. Niu, X. Zhang, et al., LncRNA BCYRN1 inhibits glioma tumorigenesis by competitively binding with miR-619-5p to regulate CUEDC2 expression and the PTEN/AKT/p21 pathway, Oncogene 39 (2020) 6879–6892.
[41] Y. Zhang, Y. Zhao, X. Ao, et al., The role of non-coding RNAs in alzheimer's disease: from regulated mechanism to therapeutic targets and diagnostic biomarkers, Front. Aging Neurosci. 13 (2021) 654978.
[42] R. Herrero, D.A. Leon, A. Gonzalez, A one-dimensional parameter-free model for carcinogenesis in gene expression space, Sci. Rep. 12 (2022) 4748.
[43] M.T.C. Poon, C.L.M. Sudlow, J.D. Figueroa, et al., Longer-term ($\geq$ 2 years) survival in patients with glioblastoma in population-based studies pre- and post-2005: a systematic review and meta-analysis, Sci. Rep. 10 (2020) 11622.
[44] H. Ohgaki, P. Kleihues, Epidemiology and etiology of gliomas, Acta Neuropathol. 109 (2005) 93.
[45] Alzheimer's Association, 2023 Alzheimer's disease facts and figures, Alzheimers Dement 19 (2023) 1598.
[46] K.H. Strang, T.E. Golde, B.I. Giasson, MAPT mutations, tauopathy, and mechanisms of neurodegeneration, Lab. Invest. 99 (7) (2019) 912–928.
[47] J. Tcw, A.M. Goate, Genetics of β-amyloid precursor protein in alzheimer's disease, Cold Spring Harb. Perspect. Med. 7 (6) (2017) a024539.
[48] A.C. Raulin, S.V. Doss, Z.A. Trottier, et al., ApoE in Alzheimer's disease: pathophysiology and therapeutic strategies, Mol. Neurodegeneration 17 (2022) 72.
[49] A.L. Cohen, S.L. Holmen, H. Colman, IDH1 and IDH2 mutations in gliomas, Curr. Neurol. Neurosci. Rep. 13 (5) (2013) 345.
[50] W.J. Chen, D.S. He, R.X. Tang, et al., Ki-67 is a valuable prognostic factor in gliomas: evidence from a systematic review and meta-analysis, Asian Pac. J. Cancer Prev. 16 (2) (2015) 411–420.

[51] S. Haase, M.B. Garcia-Fabiani, S. Carney, et al., Mutant ATRX: uncovering a new therapeutic target for glioma, Expert Opin. Ther. Targets 22 (7) (2018) 599–613.
[52] B. van Lengerich, L. Zhan, D. Xia, et al., A TREM2-activating antibody with a blood-brain barrier transport vehicle enhances microglial metabolism in Alzheimer's disease models, Nat. Neurosci. 26 (3) (2023) 416–429.
[53] R. Sun, R. Han, C. Maccornack, et al., TREM2 inhibition triggers antitumor cell activity of myeloid cells in glioblastoma, Sci. Adv. 9 (2023) eade3559.
[54] P. Mencke, et al., Bidirectional relation between Parkinson's disease and glioblastoma multiforme, Front. Neurol. 11 (2020) 898.